

# Ceramic Materials for Energy Applications II

Ceramic Engineering and Science Proceedings

Volume 33, Issue 9, 2012

*Edited by*

*Kevin Fox*

*Yutai Katoh*


*Hua-Tay Lin*

*Ilias Belharouak*

*Volume Editors*

*Michael Halbig*

*Sanjay Mathur*

 **WILEY**

The  
American  
Ceramic  
Society





---

# Ceramic Materials for Energy Applications II

---

---



# Ceramic Materials for Energy Applications II

---

*A Collection of Papers Presented at the  
36th International Conference on Advanced  
Ceramics and Composites  
January 22–27, 2012  
Daytona Beach, Florida*

Edited by  
Kevin Fox  
Yutai Katoh  
Hua-Tay Lin  
Ilias Belharouak

Volume Editors  
Michael Halbig  
Sanjay Mathur



 **WILEY**

A John Wiley & Sons, Inc., Publication

Copyright © 2013 by The American Ceramic Society. All rights reserved.

Published by John Wiley & Sons, Inc., Hoboken, New Jersey.  
Published simultaneously in Canada.

No part of this publication may be reproduced, stored in a retrieval system, or transmitted in any form or by any means, electronic, mechanical, photocopying, recording, scanning, or otherwise, except as permitted under Section 107 or 108 of the 1976 United States Copyright Act, without either the prior written permission of the Publisher, or authorization through payment of the appropriate per-copy fee to the Copyright Clearance Center, Inc., 222 Rosewood Drive, Danvers, MA 01923, (978) 750-8400, fax (978) 750-4470, or on the web at [www.copyright.com](http://www.copyright.com). Requests to the Publisher for permission should be addressed to the Permissions Department, John Wiley & Sons, Inc., 111 River Street, Hoboken, NJ 07030, (201) 748-6011, fax (201) 748-6008, or online at <http://www.wiley.com/go/permission>.

**Limit of Liability/Disclaimer of Warranty:** While the publisher and author have used their best efforts in preparing this book, they make no representations or warranties with respect to the accuracy or completeness of the contents of this book and specifically disclaim any implied warranties of merchantability or fitness for a particular purpose. No warranty may be created or extended by sales representatives or written sales materials. The advice and strategies contained herein may not be suitable for your situation. You should consult with a professional where appropriate. Neither the publisher nor author shall be liable for any loss of profit or any other commercial damages, including but not limited to special, incidental, consequential, or other damages.

For general information on our other products and services or for technical support, please contact our Customer Care Department within the United States at (800) 762-2974, outside the United States at (317) 572-3993 or fax (317) 572-4002.

Wiley also publishes its books in a variety of electronic formats. Some content that appears in print may not be available in electronic formats. For more information about Wiley products, visit our web site at [www.wiley.com](http://www.wiley.com).

***Library of Congress Cataloging-in-Publication Data is available.***

ISBN: 978-1-118-20599-0

ISSN: 0196-6219

Printed in the United States of America.

10 9 8 7 6 5 4 3 2 1

---

# Contents

---

---

Preface	vii
Introduction	ix
Analytical Techniques for Li-S Batteries Manu U. M. Patel, Rezan Demir Cakan, Mathieu Morcrette, Jean-Marie Tarascon, Miran Gaberscek, and Robert Dominko	1
Three New Approaches using Silicon in Three Valuable Energy Applications John Carberry	11
Processing of Inert SiC Matrix with TRISO Coated Fuel by Liquid Phase Sintering Kazuya Shimoda, Tatsuya Hinoki, Kurt A. Terrani, Lance L. Snead, and Yutai Katoh	25
SiC-Coated HTR Fuel Particle Performance Michael J. Kania, Heinz Nabielek, and Karl Verfondern	33
Study of the Silicon Carbide Matrix Elaboration by Film Boiling Process Aurélie Serre, Joëlle Blein, Yannick Pierre, Patrick David, Fabienne Audubert, Sylvie Bonnamy, and Eric Bruneton	71
Processing of Ultrafine Beta-Silicon Carbide Powder by Silicon–Carbon Reaction S. Sonak, S. Ramanathan, and A. K. Suri	85
Characterization of Failure Behavior of Silicon Carbide Composites by Acoustic Emission Takashi Nozawa, Kazumi Ozawa, and Hiroyasu Tanigawa	95

Recession of Silicon Carbide in Steam under Nuclear Plant LOCA Conditions up to 1400 °C Greg Markham, Rodney Hall, and Herbert Feinroth	111
The Effect of Temperature and Uniaxial Pressure on the Densification Behavior of Silica Aerogel Granules J. Matyáš, M. J. Robinson, and G. E. Fryxell	121
Microstructural Analysis of Nuclear Grade Graphite Materials Kentaro Takizawa, Toshiaki Fukuda, Akira Kondo, Yutai Katoh, and G. E. Jellison	133
A Model for Simulation of Coupled Microstructural and Compositional Evolution Veena Tikare, Eric R. Homer, and Elizabeth A. Holm	145
Characterisation of Corrosion of Nuclear Metal Wastes Encapsulated in Magnesium Silicate Hydrate (MSH) Cement Tingting Zhang, Chris Cheeseman, and Luc J. Vandeperre	159
Impact of Uranium and Thorium on High TiO <sub>2</sub> Concentration Nuclear Waste Glasses Kevin M. Fox and Thomas B. Edwards	169
Author Index	181



---

# Preface

---

---

This proceedings issue contains contributions from three energy related symposia and the European Union–USA Engineering Ceramics Summit that were part of the 36th International Conference on Advanced Ceramics and Composites (ICACC), in Daytona Beach, Florida, January 22-27, 2012. The symposia include Ceramics for Electric Energy Generation, Storage and Distribution; Advanced Ceramics and Composites for Nuclear and Fusion Applications; and Advanced Materials and Technologies for Rechargeable Batteries. These symposia and the Summit were sponsored by the ACerS Engineering Ceramics Division. The symposium on Advanced Ceramics and Composites for Nuclear and Fusion Applications was cosponsored by the ACerS Nuclear & Environmental Technology Division.

The editors wish to thank the authors and presenters for their contributions, the symposium organizers for their time and labor, and all the manuscript reviewers for their valuable comments and suggestions. Acknowledgment is also due for financial support from the Engineering Ceramics Division, the Nuclear & Environmental Technology Division, and The American Ceramic Society. The editors wish to thank Greg Geiger at ACerS for all his effort in assembling and publishing the proceedings.

KEVIN FOX, Savannah River National Laboratory  
YUTAI KATOH, Oak Ridge National Laboratory  
HUA-TAY LIN, Oak Ridge National Laboratory  
ILIAS BELHAROUAK, Argonne National Laboratory



---

# Introduction

---

---

This issue of the Ceramic Engineering and Science Proceedings (CESP) is one of nine issues that has been published based on content presented during the 36th International Conference on Advanced Ceramics and Composites (ICACC), held January 22–27, 2012 in Daytona Beach, Florida. ICACC is the most prominent international meeting in the area of advanced structural, functional, and nanoscopic ceramics, composites, and other emerging ceramic materials and technologies. This prestigious conference has been organized by The American Ceramic Society's (ACerS) Engineering Ceramics Division (ECD) since 1977.

The 36th ICACC hosted more than 1,000 attendees from 38 countries and had over 780 presentations. The topics ranged from ceramic nanomaterials to structural reliability of ceramic components which demonstrated the linkage between materials science developments at the atomic level and macro level structural applications. Papers addressed material, model, and component development and investigated the interrelations between the processing, properties, and microstructure of ceramic materials.

The conference was organized into the following symposia and focused sessions:

Symposium 1	Mechanical Behavior and Performance of Ceramics and Composites
Symposium 2	Advanced Ceramic Coatings for Structural, Environmental, and Functional Applications
Symposium 3	9th International Symposium on Solid Oxide Fuel Cells (SOFC): Materials, Science, and Technology
Symposium 4	Armor Ceramics
Symposium 5	Next Generation Bioceramics

Symposium 6	International Symposium on Ceramics for Electric Energy Generation, Storage, and Distribution
Symposium 7	6th International Symposium on Nanostructured Materials and Nanocomposites: Development and Applications
Symposium 8	6th International Symposium on Advanced Processing & Manufacturing Technologies (APMT) for Structural & Multifunctional Materials and Systems
Symposium 9	Porous Ceramics: Novel Developments and Applications
Symposium 10	Thermal Management Materials and Technologies
Symposium 11	Nanomaterials for Sensing Applications: From Fundamentals to Device Integration
Symposium 12	Materials for Extreme Environments: Ultrahigh Temperature Ceramics (UHTCs) and Nanolaminated Ternary Carbides and Nitrides (MAX Phases)
Symposium 13	Advanced Ceramics and Composites for Nuclear Applications
Symposium 14	Advanced Materials and Technologies for Rechargeable Batteries
Focused Session 1	Geopolymers, Inorganic Polymers, Hybrid Organic-Inorganic Polymer Materials
Focused Session 2	Computational Design, Modeling, Simulation and Characterization of Ceramics and Composites
Focused Session 3	Next Generation Technologies for Innovative Surface Coatings
Focused Session 4	Advanced (Ceramic) Materials and Processing for Photonics and Energy
Special Session	European Union – USA Engineering Ceramics Summit
Special Session	Global Young Investigators Forum

The proceedings papers from this conference will appear in nine issues of the 2012 Ceramic Engineering & Science Proceedings (CESP); Volume 33, Issues 2-10, 2012 as listed below.

- Mechanical Properties and Performance of Engineering Ceramics and Composites VII, CESP Volume 33, Issue 2 (includes papers from Symposium 1)
- Advanced Ceramic Coatings and Materials for Extreme Environments II, CESP Volume 33, Issue 3 (includes papers from Symposia 2 and 12 and Focused Session 3)
- Advances in Solid Oxide Fuel Cells VIII, CESP Volume 33, Issue 4 (includes papers from Symposium 3)
- Advances in Ceramic Armor VIII, CESP Volume 33, Issue 5 (includes papers from Symposium 4)

- Advances in Bioceramics and Porous Ceramics V, CESP Volume 33, Issue 6 (includes papers from Symposia 5 and 9)
- Nanostructured Materials and Nanotechnology VI, CESP Volume 33, Issue 7 (includes papers from Symposium 7)
- Advanced Processing and Manufacturing Technologies for Structural and Multifunctional Materials VI, CESP Volume 33, Issue 8 (includes papers from Symposium 8)
- Ceramic Materials for Energy Applications II, CESP Volume 33, Issue 9 (includes papers from Symposia 6, 13, and 14)
- Developments in Strategic Materials and Computational Design III, CESP Volume 33, Issue 10 (includes papers from Symposium 10 and from Focused Sessions 1, 2, and 4)

The organization of the Daytona Beach meeting and the publication of these proceedings were possible thanks to the professional staff of ACerS and the tireless dedication of many ECD members. We would especially like to express our sincere thanks to the symposia organizers, session chairs, presenters and conference attendees, for their efforts and enthusiastic participation in the vibrant and cutting-edge conference.

ACerS and the ECD invite you to attend the 37th International Conference on Advanced Ceramics and Composites (<http://www.ceramics.org/daytona2013>) January 27 to February 1, 2013 in Daytona Beach, Florida.

MICHAEL HALBIG AND SANJAY MATHUR  
 Volume Editors  
*July 2012*



## ANALYTICAL TECHNIQUES FOR Li-S BATTERIES

Manu U.M. Patel, Rezan DEMIR CAKAN, Mathieu MORCLETTE, Jean-Marie TARASCON, Miran GABERSCEK, Robert DOMINKO

National Institute of Chemistry, Hajdrihova 19, SI-1000 Ljubljana, Slovenia  
ALISTORE-ERI, 33 Rue Saint-Leu, 80039 Amiens, France  
LRCS, Université de Picardie Jules Verne, 33 Rue Saint-Leu, 80039 Amiens, France

### ABSTRACT

Lithium sulfur rechargeable batteries are foreseen to be used in electric vehicles in the near future. To enable their placement to the market we need to improve their reliability and cycling performance. This can be done by selective change of the chemical environment in the Li-S battery, including electrolyte (solvents and salts), different combinations of cathode composites and different additives. With an aim to understand differences between different chemical environments, suitable and reliable analytical techniques that can effectively monitor the changes of interest, should be developed. In this work we present two newly developed analytical techniques which are capable to detect quantitative and qualitative differences between different polysulfide species in the electrolyte. More specifically, both proposed techniques can detect the polysulfides that have diffused away from the cathode composite. With a modified 4-electrode Swagelok cell we can quantitatively determine the amount of such polysulfides, while an in-situ UV-Vis cell gives us information about the composition of these polysulfides. Combining these techniques with a classical galvanostatic cycling method could lead to a better understanding, consequently, a faster tuning of Li-S battery properties.

### INTRODUCTION

The on-going and foreseen increased electrification of the transport sector, the “electromobility” revolution is one of the major driving forces for energy storage breakthroughs. Current rechargeable Li-ion batteries for electric vehicle (EV) are capable to deliver between 100 Wh/kg and 150 Wh/kg energy density, while typical consumption of a liter of gasoline produces 2500 Wh of useful work. So there is still a factor of 15 between the energy delivered by one liter of gasoline and 1 kg of battery (e.g. the autonomy of the car with similar weight that is driven by batteries is between 5-10 times shorter than with gasoline). Hence, if we want to achieve or even approach the goal of a 500 km driving range using battery powered vehicles, we need to explore new batteries that are different from the existing Li-ion technology and that offer a real step further in the energy storage<sup>1</sup>.

One of the possibilities is the lithium-sulfur battery technology, the principle of which has been known for several decades<sup>2-4</sup>, however without real commercial breakthrough. In theory, Li-S battery can fulfill all the requirements of the intelligent vehicle battery system since it possesses a high volumetric (small size) and a high gravimetric (low weight) energy density. In addition, it can be produced as a flexible, environmental friendly and cost effective cell and in theory offers a safe and a reliable operation.

Elemental sulfur as a positive electrode material in combination with lithium metal as a negative electrode material offers an attractive high-energy rechargeable cell. More specifically, assuming the whole reaction to  $\text{Li}_2\text{S}$ , the average redx voltage and the theoretical energy values of such a cell are 2.1V and 2500W/kg (or 2800Wh/l), respectively.

One of the main reasons that the Li-S system has still not reached a wide commercial availability is the not-yet-optimized function of the cathode. Over the last two decades different directions towards improved cathode architecture and chemical compositions have been proposed. One of the strategies has been a special cell configuration where all polysulfides are solubilized – the so called catholyte cells<sup>2</sup>. Another strategy is the use of either a mixture of sulfur and suitable matrix to

improve the electronic conductivity or embedment of sulfur into a polymer matrix (for instance polyaniline).

The first discharge of Li-S battery and potential reactions are shown in the Figure 1. Along the high voltage plateau (2,3 – 2,4V), reduction of cyclic sulfur to the long chain polysulfides (e.g.  $\text{Li}_2\text{S}_8$  and  $\text{Li}_2\text{S}_6$ ) occurs. Further reduction progressively leads to the low voltage plateau at 2,1V and to the formation of  $\text{Li}_2\text{S}_4$ . The plateau at 2,1V corresponds to a 1 electron reaction per sulfur atom and to the reduction to  $\text{Li}_2\text{S}_2$ . Reduction of lithium disulfide to lithium monosulfide occurs in region C (Figure 1) and leads to a very fast voltage decay due to insolubility of  $\text{Li}_2\text{S}$  in most of electrolytes (due to the formation of insoluble blocking layer of  $\text{Li}_2\text{S}$ ).

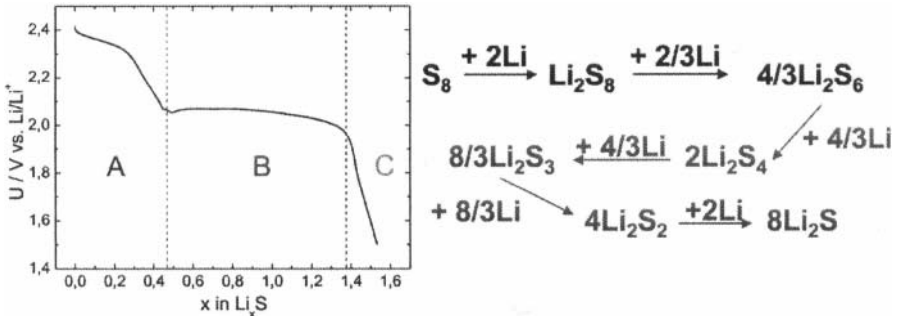


Figure 1: First discharge curve for Li-S battery and suggested reaction scheme divided into three typical regions of sulfur reduction

Regarding the chemical environment, most of polysulfides (except  $\text{Li}_2\text{S}$ ) are soluble in electrolytes and can diffuse away from the cathode composite, thus leading to active material loss and self-discharge. Once dissolved in the electrolyte, they can move to the negative electrode (metallic lithium) and react with it, leading to a shuttle mechanism that decreases charge efficiency and leads to the formation of blocking  $\text{Li}_2\text{S}$  layer on the surface of lithium. With an aim to minimize the diffusion of soluble polysulfides from the cathode composite, different strategies have been proposed. The most promising direction of cathode composite architecture is the use of mesoporous matrix with a tiny layer of sulfur dispersed on the surface of pores. Pores in this case can act as mini chambers and at least in the formation cycles the diffusion of polysulfides is reduced and postponed to later stages of Li-S battery cycling. Nevertheless, mesoporous substrate represents a high surface area substrate for sulfur impregnation. The other possible solutions how to prevent diffusion of reduced states of sulfur are the use of different electrolyte combinations or the use of different additives in the electrolyte. The common point in all of the literature reports on that matter is the lack of detailed understanding about how different changes in the chemical environment (changes in the composition and architecture of cathode composite, changes in the electrolyte formulation, etc.) affect the electrochemical performance (utilization of sulfur and discharge/charge efficiency).

Whereas most of the published works focus predominantly on the cycling behavior, efficient progress is only possible if one deeply understands the correlation between the morphological and compositional changes on one side and the electrochemistry on the other. In our recent work<sup>5</sup>, we have proposed the use of a modified 4-electrode Swagelok cell that can be used as a reliable analytical cell for the quantitative determination of polysulfides that have diffused away from cathode composite.



## EXPERIMENTAL

Cathode composites (carbon + sulfur in 1:1 weight ratio) were prepared by infiltration of sulfur onto the carbon black (Printex XE2) surface or into the mesoporous carbon. Cathode composites were mixed with 7 wt.% of PVdF (Aldrich) and additional 8 wt.% of Printex XE2 carbon black and casted on an aluminum current collector. Electrodes with diameter 12 mm containing 2-3 mg of sulfur were pressed and dried at 90°C overnight before use.

Electrolyte solutions used in this study were 1M LiTFSI (lithium bis(trifluorimethanesulfonyl)imide) containing tetra methylene sulphone (TMS) or ethyl methyl sulphone (EMS). Electrolyte solutions with chemically synthesized polysulfides were prepared by mixing adequate amount of polysulfide powder with electrolyte solutions. Polysulfide powder was prepared by reaction of stoichiometric amounts of sulfur and lithium in ethylene glycol diethyl ether at 150°C. The denotation of polysulfides is based on the stoichiometric composition and it is not necessary to reflect exact electronic state of sulfur. Chemically synthesized polysulfides, which were used for standardization, were dissolved in electrolyte to form known concentration in the electrolyte. 1mM, 5mM, 10mM, 25mM and 50mM solutions were prepared by dissolving following  $\text{Li}_2\text{S}_n$  polysulfides ( $n=2, \dots, 8$ ).

The principle of 4 electrode Swagelok cell operation was published in our previous work<sup>6</sup>. The cell comprises two electrochemical cells in one, where one serves as a typical battery cell using two electrode cells (a working electrode with casted cathode composite and lithium as counter and reference electrodes). The second one is built perpendicularly to the battery sandwich and placed in between two separators, where nickel or stainless steel wires can be used as a working electrode and platinum wire as a counter and as a reference electrode. Operation of two cells is in the sequence, i.e. galvanostatic discharging with a C/20 rate for 2h of Li-S battery followed by a cyclovoltametric measurement using perpendicular electrodes in the potential region between 2.5 and 1 V with a scan rate of  $2 \text{ mVs}^{-1}$  and continued with galvanostatic discharging. Measurements with different concentration of  $\text{Li}_2\text{S}_8$  were performed in the same way as in ordinary Li-S battery cells, except that the cathode composite did not contain any sulfur.

The cell designed for the in-situ UV-Vis measurements is based on the coffee bag cell with a sealed quartz window on one side. The cell was mounted in the UV-Vis spectrophotometer and measured simultaneously in the reflection mode during galvanostatic cycling. Charge/discharge rate was C/20 and UV-Vis spectra were measured every 15 min. Battery was built by using pressed electrode composite on the aluminum substrate, separator and ring based lithium electrode as a counter electrode. Design of ring based electrode is necessary for the detection of polysulfides in the separator in the reflection mode. Electrolyte solutions with a known concentration of different polysulfides –  $\text{Li}_2\text{S}_n$  ( $n=2-8$ ) were used for the calibration. UV-Vis spectra were measured in the cell designed for the electrochemical measurements (cell with a quartz window), except that only a separator with a wiped 1 mL of electrolyte solution containing different polysulfides was used.

## RESULTS AND DISCUSSION

The applicability of modified 4-electrode Swagelok cell was tested first in the configuration of a blank cell (cathode composite without sulfur). The corresponding cyclic voltammogram (Fig. 2a) shows a cathodic peak at a potential below 0.8 V versus platinum reference electrode. Once polysulfide solution of  $\text{Li}_2\text{S}_8$  and electrolyte are used, another cathodic peak appears in the potential range between 2.25V and 1.5V (Figure 2a). The height of this cathodic peak is in correlation with the concentration of  $\text{Li}_2\text{S}_8$  in the electrolyte. As we showed in our previous work, the correlation is linear and in some standardized conditions it can be used for comparison of different systems. However, it cannot be used for the determination of overall quantity of polysulfides that has diffused away from the cathode composite. The cumulative (integrated) charge that corresponds to the area in the selected potential range corresponds to the reduction of only approximately 2% of polysulfides added to the

electrolyte solution. Using the blank cell, we further observed that most of the polysulfides were reduced in the first scan, as shown in Figure 2b. The integrated charge in higher cycles corresponds to less than 5 % of the charge obtained from the first scan and it can be correlated to the polysulphides diffused from the rest of separator area. Typically we found a yellow to white precipitate in the separator which was in the vicinity of the working electrode (nickel or stainless steel wire), while the wire was not covered by any visible layer.

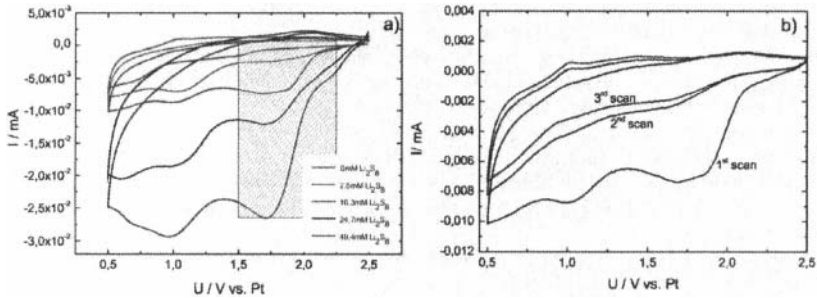


Figure 2: a) cyclic voltammograms for electrolytes in the blank battery configuration with different standards (different concentration of dissolved  $\text{Li}_2\text{S}_8$ ) and b) consecutive three cyclic voltammogram scans for the same blank battery with standard electrolyte containing 24.7 mM  $\text{Li}_2\text{S}_8$ .

Application of the modified 4-electrode cell in combination with a real battery (cathode composite containing sulfur) confirmed our expectation that we can detect polysulfides during the battery operation. Cyclic voltammograms were collected after every 2 hours of galvanostatical discharging in the first cycle (Figure 3).

The measured cyclic voltammograms showed evolution of the soluble polysulfides which can be scaled with the intensity of cathodic peak at approximately 1.8 V. Note that a remarkable change is only observed in the cathodic peak at 1.8 V while the second cathodic peak (at 1.3 V) remained relatively constant; the origin of the latter is not clear at the present state of the work. The maximum solubility has been detected after a change in the composition for  $\Delta x = 0.2$ . During the next two steps it remained relatively high. Here we need to consider that we might need to reduce shorter polysulfides ( $\text{Li}_2\text{S}_6$  and/or  $\text{Li}_2\text{S}_4$ ) chains which can consume less charge than  $\text{Li}_2\text{S}_8$  available in the beginning of the discharge curve. Later during the discharge, the amount of charge used for the reduction of soluble polysulfides becomes smaller which may be ascribed to a smaller diffusivity of shorter chain polysulfides and a smaller quantity of charge required for the reduction of short chain polysulfides (i.e. for the reduction of  $\text{Li}_2\text{S}_3$  and  $\text{Li}_2\text{S}_2$ ).

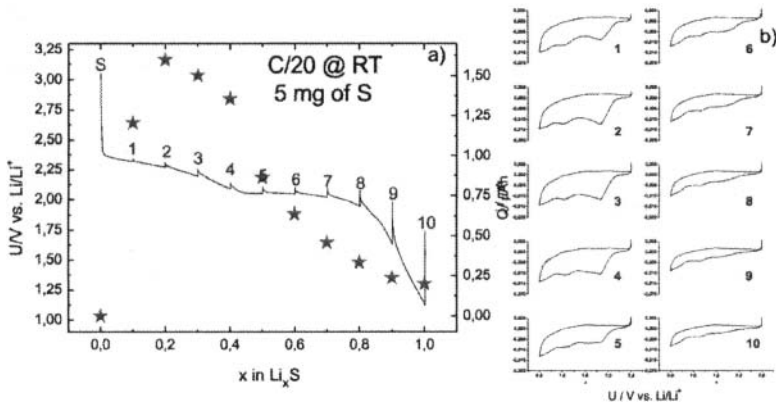


Figure 3: a) Electrochemical behavior during first reduction of Printex XE2/S composite and b) corresponding cyclic voltammograms measured after the change in composition of  $\Delta x=0,1$ . Red stars in (a) correspond to the charge obtained by integration between 2.25 and 1.5V in measured CV's.

As proposed in our previous work, various chemical environments with different electrochemical behavior showed differences in the potential region between 2.25 V and 1.5 V (changes in the integrated charge). Observed unique responses can be explained by knowing the physical and chemical properties of components used in the electrochemical cell. For instance in Figure 4 we show the starting CVs from four different chemical environments and the CVs at maximum solubility (the highest intensity of the cathodic peak at 1.8V). As expected, the battery in which we used the electrolyte containing dissolved chemically synthesized  $\text{Li}_2\text{S}_8$  showed the highest response (Figure 4a – red curve) in the first scan - even before we started with the battery (the concentration of dissolved polysulfides was about 25 mM). Other examples presented in Figure 4a show only the cathodic peak at 1.3 V and we can observe the pronounced difference between the two electrolytes (for the EMS electrolyte, the cathodic peak was observed at potentials that were for several tens of millivolts higher than in the case of the TMS electrolyte; however, one also needs to stress that the shape of CV in this region is different for mesoporous carbon compared to carbon black). Figure 4b shows cyclic voltammograms obtained during the sequenced scans, as shown in Figure 3. In this case, as presented in Figure we observed the cathodic peak at approximately 1,8V however not in all examples at the same composition ( $\Delta x$ ). Note that the highest integrated charge, as well the highest cathodic peak, was obtained with the battery where we added chemically synthesized polysulfides into the electrolyte. Surprisingly, a very high integrated charge was also obtained in the case when we used EMS as a solvent for the electrolyte. Here we need to add that this CV scan was measured in the middle of the cycling curve (not shown in this work) while using the TMS solvent for the electrolyte solution we observed the maximum intensity peak during the first plateau at 2.4V. That phenomenon can be probably explained with different viscosities of electrolytes. The difference in the results obtained with mesoporous carbon if compared to the ones obtained with a carbon black substrate (Printex XE2) is more or less expected; however, it is important that also in the case of mesoporous carbon we detected polysulphides that diffused away from the cathode composite.

Examples presented in this work show clearly that the use of modified 4-electrode Swagelok cell can help to better understand the electrochemical behavior (capacity fading and efficiency) of Li-S battery configuration. For example, recently we have shown that when oxide based substrates were

used as a substrate for sulfur impregnation', the capacity fading was slower than in the case where mesoporous carbon was used. However, the formation was comparable in both cases. This unexpected result was explained by the use of 4-electrode Swagelok cell where we detected a much lower cathodic peak during the operation of battery containing oxide based substrate in the cathode composite. The reason for the smaller detected amount of polysulfides was not due to the more efficiently confined sulfur in the pores of SBA-15 but due to the weak bonding between pores and formed polysulfides. Modified 4-electrode Swagelok cell can be used as a reliable analytical cell for Li-S batteries where we can quantitatively determine the amount of polysulfides that diffuse away from the cathode composite.

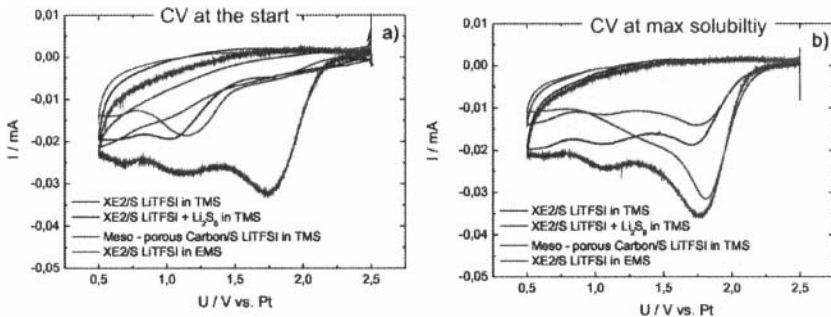


Figure 4: a) CV scans of different Li-S batteries obtained before galvanostatic discharge and b) CV scans obtained during the sequenced scans measured during galvanostatic discharge where we observed the highest peak at 1,8V versus Pt electrode.

The second in-situ analytical technique presented in this work uses the property of polysulfides having different colors. In this way, UV-Visible spectroscopy becomes an effective way of detecting polysulfides, both quantitatively and qualitatively. Namely, polysulfides with different chain lengths reflect back (after absorption) different amount of energy when they are exposed to UV-Visible light. Thus, shorter chain lengths reflect back light with shorter wavelength and polysulfides with longer chain length reflects back light with a few tenths on nanometer longer wavelength. The color and consequently the position of spectra is a function, besides the chain length, also of the alkali metal in polysulfides and the medium where polysulfides are dissolved, while the intensity of the color is a function of the concentration. Lithium polysulfides dissolved in 1 M LiTFSI TMS electrolyte showed different colors going from reddish-brown for the dissolved long chain polysulfides to green-yellow color for short chain polysulfides.

UV-Vis spectra presented in Figure 5 were obtained in-situ during the galvanostatical discharge and charge of a Li-S battery that was mounted in UV-Vis spectrometer. Spectra were measured in the sequence of every 15 minutes (sequence of spectra changes from green to violet color in Figure 5). Clear reflection from the black surface can be observed in the beginning with no reflection in the visible light region. During discharge, polysulfides were formed and the shape of UV-Vis spectra changed due to non-transparent nature of separator once it contained dissolved polysulfides. These changes are continuous until the maximum concentration and further discharging leads to the formation of the shorter chain polysulfides which differ also in the shape of UV-Vis spectra. Interestingly, during charge the changes are less pronounced since polysulfides remain in the separator and - following colors from green through pink to violet - one can see the polysulfide shuttle mechanism. In the start of discharging the position of the derivative peak in the visible light region is below 500 nm which suggests the presence of short chain polysulfides. With charging it shifts to higher wavelengths which could be interpreted as oxidation of short chain polysulfide to long chain polysulfides, but at the end of